Astronomical Techniques and Instruments, Vol. 2, May 2025, 127–147

Review Open Access

A review of deep learning-based analyses of impact crater detection on different celestial bodies

Xu Zhang[1], Jialong Lai[1*], Feifei Cui[1], Chunyu Ding[2], Zhicheng Zhong[1]

[1]*School of Science*, *Jiangxi University of Science and Technology*, *Ganzhou* 341000, *China*

[2]*Institute for Advanced Study*, *Shenzhen University*, *Shenzhen* 518000, *China*

*Correspondence: laijialong@jxust.edu.cn

Received: December 10, 2024; Accepted: February 21, 2025; Published Online: April 7, 2025; https://doi.org/10.61977/ati2024068; https://cstr.cn/32083.14.ati2024068

Citation: Zhang, X., Lai, J. L., Cui, F. F., et al. 2025. A review of deep learning-based analyses of impact crater detection on different celestial bodies. *Astronomical Techniques and Instruments*, **2**(3): 127−147. https://doi.org/10.61977/ati2024068.

Abstract: Planetary surfaces, shaped by billions of years of geologic evolution, display numerous impact craters whose distribution of size, density, and spatial arrangement reveals the celestial body's history. Identifying these craters is essential for planetary science and is currently mainly achieved with deep learning-driven detection algorithms. However, because impact crater characteristics are substantially affected by the geologic environment, surface materials, and atmospheric conditions, the performance of deep learning models can be inconsistent between celestial bodies. In this paper, we first examine how the surface characteristics of the Moon, Mars, and Earth, along with the differences in their impact crater features, affect model performance. Then, we compare crater detection across celestial bodies by analyzing enhanced convolutional neural networks and U-shaped Convolutional Neural Network-based models to highlight how geology, data, and model design affect accuracy and generalization. Finally, we address current deep learning challenges, suggest directions for model improvement, such as multimodal data fusion and cross-planet learning and list available impact crater databases. This review can provide necessary technical support for deep space exploration and planetary science, as well as new ideas and directions for future research on automatic detection of impact craters on celestial body surfaces and on planetary geology.

Keywords: Crater detection algorithms; Deep learning; Different celestial bodies; Impact crater databases

1. INTRODUCTION

Impact craters are among the most prevalent geological features in the solar system, formed sporadically on long timescales by asteroid impacts on the surfaces of planets or moons and by collisions with other celestial bodies. The formation of impact craters not only constitutes a prominent geomorphological feature on the surface of many planets but also profoundly influences the process of planetary formation and evolution[1]. Whether on the Moon, Mars, or other terrestrial bodies, the impact craters on their surfaces record the results of celestial interactions, and the morphological features, formation mechanisms, and distribution patterns of impact craters provide valuable insights for studying planetary geological evolution, atmospheric history, and celestial collisions[2]. Additionally, they are crucial for understanding the origin and evolution of planets in the solar system, planning deep space exploration missions, and investigating potential conditions for the origin of life[3]. Therefore, the study of impact crater detection holds an essential place in the field of planetary science.

Established impact crater detection methods are divided into manual labeling methods and automated algorithms relying on the geometric features of impact craters. Manual labeling is the earliest detection method, in which researchers manually mark the boundaries of impact craters in images and calculate relevant parameters such as diameter and depth by observing remote sensing images or digital elevation models (DEMs)[4] of planetary surfaces. Most of the early impact crater databases for objects such as the Moon and Mars were constructed manually[5,6] and although this method has been successful in initial research, there are often notable differences in the labeling results from different researchers because of the extraordinarily time-consuming and subjective nature of the manual labeling process[7,8], with discrepancies reaching as high as 40%[8–10]. Automated methods have gradually been introduced to address these problems and improve research efficiency. Traditional automated methods are typically on the basis of the morphologi-

cal features of impact craters, such as annular boundaries and depressed topography, which are recognized using image processing techniques such as edge detection and morphological operations[11,12]. Additionally, techniques combining DEMs and optical imagery can improve detection accuracy by analyzing terrain undulation and slope features[13,14]. However, these methods have high requirements regarding the shape of impact craters and have room for improvement when dealing with complex backgrounds, such as Martian dust-covered areas and in identifying small impact craters, which are easily affected by light variations and noise. As a result, they are not effective in dealing with overlapping craters or eroded impact craters[15]. Overall, traditional methods have limitations in terms of efficiency, accuracy, and adaptability, which make it challenging to handle the large volumes of high-resolution data generated by current planetary exploration missions and to adapt to the notable geological differences across different celestial surfaces[7,16]. Because deep learning methods offer a high degree of automation and adaptability to diverse environments, they can effectively overcome the limitations faced by earlier methods in impact crater detection. Consequently, deep learning has gradually become an essential tool in impact crater detection.

In recent years, researchers have developed many impact crater detection algorithms (CDAs) on the basis of deep learning techniques, which have proven effective at solving many problems associated with more traditional methods for identifying impact craters on planetary surfaces. Compared with manual labeling methods and automated methods on the basis of the geometric features of impact craters, deep learning possesses powerful feature extraction and nonlinear modeling capabilities, which enable the automatic detectionof impact craters from complex and diverse data, markedly improving the efficiency and accuracy of detection [1,17]. For example, deep learning models on the basis of system architecture such as convolutional neural networks (CNNs) can automatically capture the boundaries, shape features, and background environment of impact craters, accurately identifying craters of different scales and morphologies through multi-layer feature extraction[18,19]. Additionally, deep learning models can flexibly adapt to different data sources (e.g., optical images, DEMs, and multispectral data) and geological conditions on a variety of celestial surfaces, effectively addressing the adaptability issues of previous methods in cross-celestial studies[16,20]. Thanks to their efficient end-to-end learning capability, the training and inference speed of deep learning techniques on large-scale datasets is considerably faster than that of older algorithms, enabling quick processing of a large number of high-resolution images generated by planetary exploration missions[8,21]. Furthermore, through the use of data augmentation, multimodal data fusion, and transfer learning, deep learning further extends the application scenarios and adaptability of impact crater detection, making it more robust in dealing with complex backgrounds, secondary crater detection, and multi-object comparison studies[18,22]. Consequently, deep learning plays a central role in automating and improving the accuracy of impact crater detection and provides more efficient technical solutions with broader application scenarios for planetary science research.

CDAs demonstrate excellent efficiency and accuracy in data processing on a single celestial body. They provide technical support and new research perspectives for the study of impact craters on different celestial bodies, owing to their automation and ability to adapt to diverse environments. Studying impact craters on a variety of celestial bodies is of foremost importance in planetary science, because the geological environment, gravitational field, and atmospheric conditions of each body strongly affect the formation mechanism, feature preservation, and distribution patterns of impact craters. These differences offer valuable insights into the formation, evolution, and interaction of planets[7]. For example, the Moon, whose impact craters remain clear and intact for long periods because of the lack of atmospheric and geological activity, is ideal for studying impact dynamics and secondary crater distribution[23,24]. By contrast, the thin atmosphere and active wind and sand erosion on Mars lead to the erosion or masking of crater edges and its complex sediment cover and geomorphological changes make the morphological characteristics of impact craters and the distribution patterns of secondary craters appear more diverse[21,25]. On Earth, the preservation of impact craters is severely limited by geological processes such as plate tectonics, erosion, and deposition, with only a few larger impact craters remaining recognizable[26,27]. Saturn's moon Titan has few surface impact craters, mainly owing to its active geological and climatic features, such as liquid methane rivers, lakes, and wind-formed landforms, which can mask or erode impact craters. Titan's thick atmosphere also reduces the impact of many small meteors, decreasing the number of craters. Many other objects with complex surface features and unique atmospheric environments can provide new perspectives for studying the formation and evolution of impact craters[28].

Through cross-body comparative studies, researchers can uncover universal patterns in geological processes while identifying phenomena unique to different celestial bodies, thus advancing CDA automation. For example, Herd et al.[25] and Xiao et al.[29] demonstrated the notable environmental effects of surface deposition and gravity on crater morphology by comparing Martian and lunar impact craters[25,29,30]. However, challenges remain in cross-body comparative studies, including differences in the resolution and quality of remote sensing data, the complexity of crater morphology and the diversity of geological environments and formation mechanisms[19,31]. In recent years, the introduction of deep learning techniques has provided powerful tools for the automated detection and analysis of impact craters on various celestial bodies, enhancing detection efficiency and supporting the development of cross-celestial comparative studies[32,33].

The study of impact craters on different celestial bodies is essential to planetary science, not only for understanding the geological evolution and surface chronology of planets but also for providing technical support and a scientific foundation for future deep space exploration missions. This field of research will lead to new discoveries and insights into geological history, material cycles, and celestial interactions, offering more opportunities to understand the evolutionary processes of the solar system[34,35].

In this paper, we explore the application and performance of deep learning techniques in impact crater detection on the surfaces of different celestial bodies and evaluates the adaptability and detection capabilities of deep learning models in multi-planet environments by analyzing impact crater detection studies on typical celestial bodies such as the Moon, Mars, and Mercury. Specifically, we compare the performance of various models across different celestial bodies and analyze the key factors affecting the generalization ability of the models. At the same time, we summarize the technical challenges in detection tasks across different celestial bodies and propose potential directions for improvement. Reviewing and summarizing existing research, we aim to provide technical support and theoretical references for future deep space exploration missions and planetary geology studies.

2. SURFACE FEATURES AND CRATER UNIQUENESS ON DIFFERENT CELESTIAL BODIES

The characteristics of impact craters on planets and moons can be influenced by various geological and physical factors, including the surface geological environment, atmospheric conditions, gravitational field strength, and the history of geological activity. Owing to marked differences in the geological conditions and physical properties of different celestial bodies, the preservation state, morphological features, and distribution patterns of impact craters also vary. This diversity can provide valuable information for studying the formation and evolution of planetary surfaces, but it also presents a challenge to the development of more accurate crater detection techniques.

2.1. Surface Features on Different Celestial Bodies

In this study, we have examined the Moon, Mars, Earth, Mercury, Enceladus, and Titan, all of which have impact craters with unique characteristics. The Moon possesses one of the largest distributions of well-preserved impact craters in the solar system. Because of its lack of atmosphere and limited geological activity, its impact crater morphology has remained largely intact, with well-defined and regular boundaries, typically round or oval. A typical example of an impact crater on the Moon is the Copernicus Crater, located on the near side of the Moon with a diameter of approximately 93 km, known for its well-defined ejecta system. Additionally, the lunar surface is extensively covered with secondary craters, originating from the secondary impacts of ejecta from large primary craters. The impact craters on the Moon record the history of effects from the early formation of the solar system to the present, making it an ideal subject for studying impact dynamics and planetary surface chronology[8,23].

Impact craters on Mars show complex and diverse morphological features influenced by its thin atmosphere and active wind and sand processes. The surface of Mars is covered with sandy sediments and ice and the edges of some impact craters are indistinct or obscured, with their interiors often covered by deposits[21]. In addition, the Martian atmosphere can form secondary craters, but the distribution pattern of these craters is influenced by geological conditions and depositional processes. These characteristics of Martian impact craters provide essential insights into depositional environments and the distribution of secondary craters[7]. A representative impact crater on Mars is Gale Crater, located near the equator, with a diameter of approximately 154 km. At its center is Mount Sharp, rising approximately 5.5 km in height. The NASA Curiosity rover landed there in 2012 and continues to explore.

The number of impact craters on Earth is small and they are poorly preserved because of the heavy atmosphere and intense geologic activity. Plate movement, erosion, and deposition have destroyed most impact craters on the Earth's surface and only a few of the larger impact craters are recognizable, such as the Barringer Crater and Lake Manicouagan. The residual morphology of Earth's impact craters is primarily complex, irregularly shaped, and often covered by sediments[26,27].

Mercury has no atmosphere, weak surface geology, and a dense and well-preserved distribution of impact craters. Its weak gravitational field facilitates the formation of multi-ring craters and secondary craters, with the Caloris Basin being a typical example. Mercury's impact craters have clear morphology with regular boundaries and are primarily circular or elliptical, suitable for studying secondary craters, impact mechanisms, and generation laws[30,36].

The polar regions of Enceladus and Titan are characterized by geologic activity and liquid hydrocarbon lakes, respectively, rather than by impact craters. The surface of Enceladus is covered by a thick crust of ice and its impact craters are sparse, but some of them show noteworthy ice-filled and frozen structures inside. Substantial geologic activity on Enceladus's surface, such as possible cryovolcanism, has resulted in some impact craters having degraded or unrecognizable morphologies. In addition, Enceladus may have a deep subsurface ocean, suggested by the presence of distinctive “tiger stripe” fissures in the south polar region, which are the source of jet plumes. Its impact crater distribution could provide clues for exploring subsurface ice and liquid water[28].

Titan has a thick atmosphere, surface rivers composed of liquid hydrocarbons (primarily methane and

ethane), and its impact craters are sparse and diverse. Hydrocarbon deposits and erosion cover most impact craters and only a sparse distribution of impact craters remains in localized areas. The NASA Cassini probe has observed Titan's north polar region in detail, finding it to be characterized by large hydrocarbon lakes and seas. Impact crater studies on Titan have provided essential data for understanding methane cycling and deposition processes[28].

Remote sensing images of typical impact craters on each planet are shown in Fig. 1. In addition, Table 1 summarizes a comparison of the impact crater characteristics for each celestial body, including the atmospheric environment, geological activity, surface impact crater morphology, distribution of secondary craters, and the names of representative impact craters on each planet.

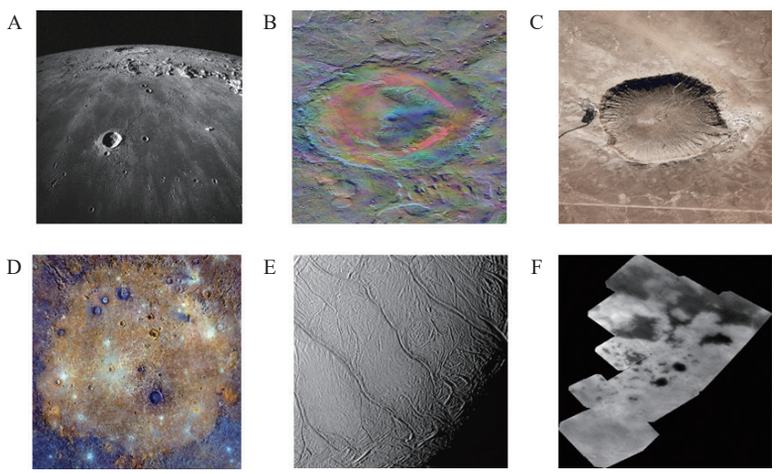

Fig. 1. Comparison of typical impact craters on various planets. (A) Moon: Copernicus Crater[1]. (B) Mars: Gale Crater in August 2012[2]. (C) Earth: Barringer Crater (Arizona, USA)[3]. (D) Mercury: Caloris Basin[4]. (E) Enceladus: polar tiger stripes (close-up view)[5]. (F) Titan: north polar "Land of Lakes" (bird's eye view)[6].

2.2. Impact Crater Uniqueness Analysis

The geological environment of planets and satellites has a profound influence on the formation, evolution, and preservation of impact craters. Geological age, geological structure, and atmospheric conditions are the central factors determining the morphology and distribution of impact craters, and these variables have diverse manifestations on different celestial bodies. The following is an in-depth discussion on how these three geological differences have shaped the characteristics of impact craters on other celestial bodies.

Regarding geological age, the history of geological activity on different celestial bodies has influenced the distribution pattern and preservation state of impact craters. Because of their low geologic activity, the Moon and Mercury have a dense distribution of well-preserved impact craters on their surfaces, which record an impact history from the early formation of the solar system to current times. The impact craters present on these objects range from small craters with diameters of only a few meters to large impact basins with diameters of more than 2500 km, providing a rich database for planetary chronology studies[7,30]. In contrast, impact craters on Mars are predominantly found in ancient upland areas with shorter period depositional environments, reflecting the effects of recent geologic activity. The covering effect of Martian regolith affects the distribution pattern of secondary craters, giving them complex spatial distribution characteristics in localized areas[36]. Most impact craters on Earth have been affected by dynamic processes such as plate tectonics, erosion, and deposition, and only a few large complex craters have been preserved[26,27]. In addition, dynamic processes on the surfaces of Enceladus and Titan have also affected the preservation of impact craters. Enceladus's ice-shell motion masks some impact craters, while Titan's sedimentary cover reduces the number of identifiable small craters, resulting in a sparse distribution[28].

In terms of geological structure, the structural composition and nature of the surfaces of celestial bodies have a strong influence on the morphology and state of preservation of impact craters. The surfaces of the Moon and Mercury are composed of stable rock, such as basalt, with

1. NASA Lunar Reconnaissance Orbiter (LRO) Gallery, Lunar and Planetary Institute.

2. NASA Mars Science Laboratory (MSL) Gallery, NASA/JPL-Caltech/ESA/DLR/FU Berlin/MSSS.

3. NASA Earth Observatory, USGS National Map Data Download and Visualization Services.

4. NASA MESSENGER Mission Gallery, NASA/Johns Hopkins University Applied Physics Laboratory/Carnegie Institution of Washington.

5. NASA Cassini Mission Gallery, NASA/JPL/Space Science Institute.

6. NASA Cassini Mission Gallery, NASA/JPL-Caltech/SSI/JHUAPL/Univ. of Arizona.

Table 1. List of celestial bodies and their impact crater characteristics

Celestial body	Atmospheric environment	Geological activity	Impact crater morphology	Secondary crater distribution	Representative impact crater
Moon[8,23]	None	Weak	Clear, regular	Dense distribution	Copernicus Crater
Mars[7,21]	Thin	Active wind and sand deposition	Deposits cover fuzzy boundaries	Complex distribution	Gale Crater
Earth[26]	Thick	Active plate tectonics	Often eroded or buried	Rare	Barringer Crater
Mercury[23,29]	None	Weak	Clear, regular, many large craters	Dense distribution	Caloris Basin
Enceladus[37]	None	Significant geological activity (ice)	Ice-filled, complex structure	Rare	Shahryar Crater
Titan[28]	Thick	Active deposition and erosion	Diverse, sediment-covered	Rare	North polar lakes

well-defined and morphologically intact impact crater boundaries, making them ideal for studying impact dynamics. The surface of Mars has a relatively complex composition of materials, including ice, regolith, and volcanic rock, and its heterogeneity makes its impact craters show diverse morphological characteristics. Enceladus's impact craters are mostly filled with icy material and show a unique frozen structure, a characteristic that reflects the role of icy crust layers in shaping the morphology of impact craters. Titan's impact craters are mainly eroded and covered by hydrocarbon lake and river sediments and their morphology is complex and varied, which further increases the difficulty in identifying impact craters.

The presence or absence of an atmosphere is an essential factor influencing the formation and distribution of impact craters. The lack of atmospheric layers on the Moon and Mercury has allowed their impact craters to maintain their original morphology for a long time, with clear and regular boundaries. The thin atmosphere of Mars enables the formation of some small impact craters, but surface deposition and wind erosion have a strong impact on the morphology of impact craters, making their edges poorly defined and their morphology irregular. Titan's thick atmosphere markedly reduces the probability of small impact crater formation; atmospheric deposition and erosion have resulted in a complex and varied impact crater distribution pattern, with some areas of the craters almost wholly obscured.

A combination of geological and environmental conditions on different celestial bodies influences the shape, size distribution, and sediment characteristics of their impact craters. Craters on the Moon and Mercury have regular shapes and clear boundaries, mostly circular or elliptical. In contrast, impact craters on Mars have indistinct or asymmetric edges due to sedimentation and wind erosion. The morphology of Enceladus's impact craters has been shaped by deposition of ice and shows unique frozen structures, while Titan's impact craters show morphological diversity due to sedimentary cover. Generally, crater characteristics reflect the geology and environment of the different celestial bodies.

Impact craters on the Moon and Mercury have a wide range of sizes and small secondary craters are densely and strongly distributed. Martian impact craters cover a wider range of scales, but the sedimentary cover makes it more challenging to recognize small and secondary craters, which are densely distributed only in certain regions. Titan's impact craters are fewer in number, dominated by large craters, with smaller craters substantially obscured by sedimentation and erosion and their distribution pattern shows a higher spatial sparsity.

Sediment characteristics further exacerbate the difficulty of impact crater classification and detection. Martian regolith deposits often form stacked structures at the base and edges of impact craters, which clearly interferes with CDAs. Liquid methane deposits on the surface of Titan mask the boundaries of impact craters, potentially making detection a challenge. These depositional features not only reflect the geological dynamics of the object's surface but also place higher demands on automated detection techniques.

Analysis of the geological properties of the Moon, Mars, Earth, Mercury, Enceladus, and Titan shows that the geological age, geological structure, and atmospheric conditions of different celestial bodies have a defining influence on the morphology and distribution of impact craters. This variety of impact crater morphology and distribution in different celestial bodies provides a rich scientific basis for the study of planetary impact craters and at the same time poses a new challenge to automated detection technology.

3. DEEP LEARNING FUNDAMENTALS

3.1. Deep Learning Concepts

Deep learning, a branch of machine learning on the basis of artificial neural networks, automatically learns and extracts features from data using multi-layer networks. These models build hierarchical data representations, from simple to complex, mimicking the structure of biological neural systems.

In impact crater detection, common deep learning models include CNNs, U-Net, and Faster Region-based CNNs (Faster R-CNN). CNNs automatically extract hierarchical features through multi-layer convolution and pooling, making them effective for analyzing crater edges and structures. However, because of their simple structure, they struggle with complex backgrounds or overlapping

craters, reducing detection accuracy. U-Net, known for image segmentation, captures multi-scale features and excels at extracting fine crater boundaries. However, it may not perform well with very small or large craters and can unduly smooth or miss boundaries in overlapping or eroded cases. Here, "unduly smooth" refers to the model's tendency to produce segmentation masks with softened crater edges—rather than sharp, well-defined contours—due to factors such as interpolation or loss of fine details during prediction, particularly when distinguishing overlapping or eroded craters is challenging. The Faster R-CNN, a target detection model, is well suited for detecting craters of various sizes by combining region proposal networks and convolutional layers. However, the preset anchor size impacts results and fine-tuning may be needed for craters at varying scales. Additionally, Faster R-CNN may face false and missed detections when handling dense or overlapping targets. In summary, each of these deep learning models has its own advantages in impact crater detection, and through flexible model selection and combination, the accuracy and efficiency of detection can be effectively improved to promote the research and development of automatic impact crater detection.

Commonly used evaluation metrics in CDAs include precision, recall, F_1-score (the harmonic mean of precision and recall), accuracy, mean average precision (mAP), and intersection-over-union (IoU). These metrics apply to different datasets, unbalanced samples, and detection scenarios and can comprehensively evaluate the performance of the model.

Precision is the proportion of predicted impact craters that are correctly identified. This metric is used to assess the accuracy of the positive samples predicted by the model and is particularly applicable to the assessment of scenarios that reduce false detections. The precision (P) can be calculated as

$$P = \frac{TP}{TP + FP}, \tag{1}$$

where true positive (TP) is the number of actual impact crater samples and false positive (FP) is the number of non-crater samples misidentified as impact craters.

Recall (R) is the proportion of all actual crater samples correctly detected by the model. It is used to assess the detection rate of the model and is a good measure of its performance in terms of completeness. This can be calculated as

$$R = \frac{TP}{TP + FN}, \tag{2}$$

where false negative (FN) denotes the number of impact craters not detected by the model. A high recall rate ensures that more impact craters are recognized, which is useful in scenarios more sensitive to missed detections.

The F_1-score is the harmonic mean of precision and recall, used to find a balance between precision and recall, especially for impact crater detection with unbalanced positive and negative samples. This can be determined as

$$F_1 = 2\frac{PR}{P + R}, \tag{3}$$

A higher F_1-score indicates that the model is better balanced regarding detection accuracy and recall.

Accuracy (A) is the ratio of the number of samples with all correct predictions to the total number of samples. In impact crater detection, Accuracy is used to assess the overall performance of the model on the entire dataset, but the metric may be less representative when the samples are unbalanced. This can be determined as

$$A = \frac{TP + TN}{TP + FP + FN + TN}, \tag{4}$$

where true negative (TN) is the number of samples correctly identified as non-impact craters.

The mAP is the mean accuracy across all detection categories and is particularly suitable for multi-target detection tasks. mAP values indicate the average detection capability of the model at different IoU thresholds and are often analyzed by generating Precision-Recall (PR) curves. Higher mAP values indicate a more substantial overall performance of the model for multi-scale impact crater detection.

IoU calculates the intersection and concurrency ratio of the predicted frame to the proper frame to assess the model's accuracy in predicting the bounding box. It can be determined as

$$IoU = \frac{A \cap B}{A \cup B}. \tag{5}$$

Here, A and B represent two bounding boxes, which can be either predicted by the model or manually labeled as ground truth. We employ the IoU value with a threshold setting (e.g., 0.5 or 0.75) to evaluate the degree of overlap between predicted and actual results. It is widely applied in target detection scenarios, especially in impact crater detection, where accurate labeling is required.

The above evaluation indices provide a detailed way of evaluating the impact crater detection model using multi-dimensional measurements of its performance. This enables the model to be optimized under different conditions, such as unbalanced samples, low false-detection rate, and high recall rate, to improve its accuracy and robustness.

3.2. Comparison with Traditional Methods

In impact crater detection, the limitations of traditional methods are increasingly highlighted in practical applications. Such methods rely on manually designated features, such as edges, shapes, and textures, which require extensive expertise in the specific field and are difficult to generalize to different datasets[17]. When dealing with complex impact crater features, these methods face many chal-

lenges, such as limited ability to cope with illumination variations, wide ranges of spatial scales, overlapping impact craters, and degradation phenomena[23]. In addition, traditional methods could improve in detecting impact craters with indistinct boundaries or severe erosion, while resolution limitations hinder the detection of small impact craters[13].

Traditional methods are more sensitive to noise, especially when there is more noise in high-resolution images, causing the detection accuracy to decrease substantially[38,39]. In addition, manual feature extraction and selection processes are inconvenient and susceptible to subjective influence, which can be inefficient and may lead to insufficient features or overfitting. When confronted with large-scale datasets, traditional methods have a greater time requirement, lower capacity for automation, and lack of transparency in the results, which further limits their practical applications[3,40].

By contrast, deep learning methods show clear advantages in feature extraction, robustness, multi-scale adaptation, and automated processing. Deep learning models strongly reduce the reliance on manually determined features and improve the generalization ability of the models by automatically learning hierarchical features[17]. In addition, these models can efficiently cope with complex conditions such as illumination variations, noise, and low resolution, while being able to adapt to changes in the size of impact craters through a multi-scale feature extraction framework[20]. Deep learning can also address the problem of scarcity of labeled data by applying pretrained models to impact crater detection on different celestial bodies using transfer learning techniques[41].

In terms of efficiency, the deep learning model relies on Graphics Processing Unit (GPU) acceleration and an end-to-end detection framework to achieve efficient processing and real-time detection of large-scale data, whereas the traditional approach performs poorly with large data volumes[42]. In summary, the advantages of deep learning in the task of impact crater detection are undeniable, especially in terms of automation, robustness, and multi-scale adaptation. However, deep learning also faces challenges, such as data labeling dependency, high computational resource requirements, and further optimization of model structure. Training strategies are needed to meet the needs of a broader range of applications.

3.3. Deep Learning Models

In impact crater detection, common deep learning models include CNNs and U-Net, which have been applied and improved in various studies to enhance accuracy, generalization, and efficiency. CNNs are widely used for impact crater detection because of their ability to extract features from image data and Cohen et al.[15] demonstrated their effectiveness in this task. A CNN extracts local features through convolutional operations, preserving spatial relationships. Its basic structure includes a convolutional layer, a pooling layer, and a fully connected layer. The convolutional layer creates feature maps by sliding a convolution kernel over the image, while the pooling layer reduces the feature map size to lower computational complexity. The fully connected layer combines the extracted features for classification or regression tasks. Nonlinear activation functions, such as a Rectified Linear Unit (ReLU), are used to enhance the expressive power of the model. By stacking convolutional, pooling, and activation layers, CNNs build hierarchical representations of image features, from low-level edges to high-level semantic features, enabling effective image classification and target detection.

In the case of the 16-layer Visual Geometry Group (VGG-16), it is a classic representative model of CNNs, which is very influential in the development history of deep learning and is often used as a baseline model for tasks such as image classification, feature extraction, and transfer learning. The input is a 224 × 224 image in RGB color. The network consists of several stacked convolutional layers, each with a 3 × 3 kernel, followed by ReLU activation functions. The feature maps are downsampled by max pooling to extract higher-level features. Three fully connected layers at the end produce the final classification output through a Softmax layer (the specific structure is shown in Fig. 2).

The convolutional and pooling layers in the structure are stacked in multiple layers to construct a hierarchical representation of the image features, layer by layer, from low-level edges to high-level semantic features. This makes VGG-16 perform well in tasks such as image classification and target detection. The design of the VGG-16 structure, which uses multiple smaller convolutional kernels instead of larger ones, helps to reduce the number of parameters and enhances the model's expressive ability.

U-Net is a family of semantic segmentation models, widely used for pixel-level classification of high-resolution images, including impact crater detection. It features a U-shaped symmetric structure with an encoding path (downsampling) and a decoding path (upsampling). As shown in Fig. 3, the encoder (left half) consists of multiple convolutional and pooling layers that reduce spatial resolution and increase feature channels, extracting deep image features. During encoding, the feature map resolution is halved, and each pooling layer increases feature dimensionality.

The decoder (right half) recovers spatial resolution through upsampling. Each upsampling step “jump-connects” the corresponding encoder feature map to the decoder, using a “copy and crop” operation that preserves high-resolution shallow features, helping to restore segmentation details. Finally, a 1 × 1 convolutional layer generates the segmentation map, matching the input resolution.

The key advantage of U-Net lies in its use of jump-connections to combine encoder and decoder features, allowing effective multi-level feature utilization. This structure is ideal for fine segmentation tasks, such as medical image segmentation and is also well suited for impact

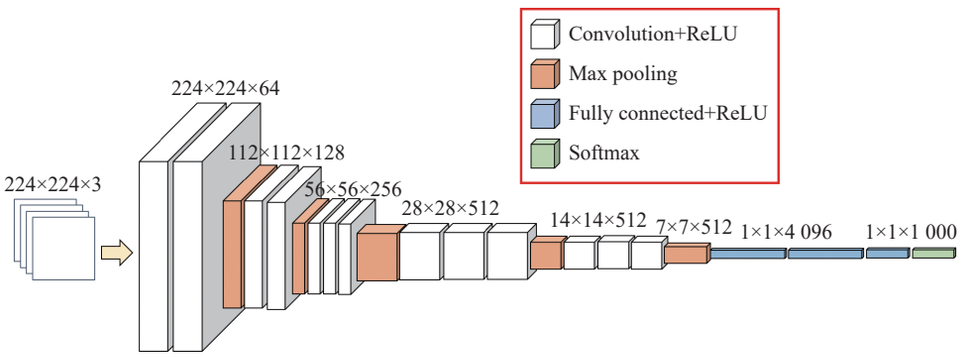

Fig. 2. Structure of a CNN, represented here by the VGG-16 model. The data cube dimensions at each processing step, from the input (224 × 224 × 3) to the final output (1 × 1 × 1 000)[43], are indicated.

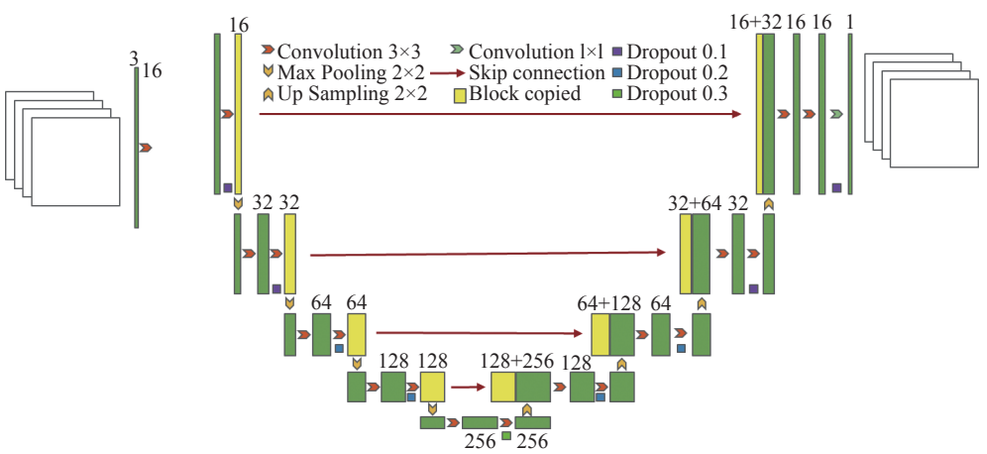

Fig. 3. U-Net architecture. This diagram illustrates the encoder–decoder structure, initialized with an input of 16 × 16 × 3 and featuring convolutional layers with 3 × 3 kernels (orange) and 1 × 1 convolution kernels (green), max pooling layers for downsampling (light yellow), and upsampling layers with 2 × 2 blocks (light yellow). Skip connections (red) enhance feature integration between the encoder and decoder, with channel dimensions increasing from 16 to 256[44].

crater segmentation.

In impact crater detection, the application of deep learning models has made notable progress and has been continuously improved to meet the needs of different detection tasks. Established deep learning models, such as CNN and U-Net, have demonstrated excellent performance in feature extraction, localization, and segmentation tasks for impact crater detection. Wang et al.[45] reported that the detection rate of the CNN-based improved model exceeds 97% for images of complex terrain and Hong et al. [46] determined that the recall rate of the U-Net-based improved model can reach 90.17%.

In recent years, transformer-based models have shown great potential because of their advantages in processing sequence data, enabling more accurate detection of impact craters. Guo et al.[47] introduced the Transformer structure and constructed the Crater Detection Transformer (Crater-DETR) model through dense supervision and multi-scale fusion techniques, which achieved an accuracy of 88.13%, and enhanced the detection of small impact craters. Zhang et al.[48] constructed the Lunar Complex Crater Retrieval Network (LC2R-Net) model by introducing the Swin Transformer and using a deep feature fusion strategy. The image retrieval accuracy of this method reached 83.75%, achieving remarkable results in the image retrieval of complex impact craters on the Moon.

Self-supervised learning (SSL) is another technique which is gradually emerging in the field of planetary science, where labeled data are scarce. Using SSL, models are able to self-learn using unlabeled data, which reduces the dependence on labeled data and improves the generalization ability on unknown data. Tejas et al.[49] applied SSL to automatic classification of unlabeled Martian topographic images and improved the accuracy of identifying topographic features and the efficiency of scientific classification through a self-supervised deep clustering algorithm. This achieved an overall accuracy of 83.6% and a retrieval accuracy of 100% in some cases.

Xiang et al.[50] used SSL to improve the processing of Mars images under the influence of dust storms, which improved the clarity and color fidelity of the images, enabling the model to achieve an average gradient and edge intensity metrics of 7.94 and 55.47, respectively, which effectively improved the quality of the images.

In the future, with the increasing amount of high-resolution data available for the surface of celestial bodies such

as the Moon and Mars and the continuous advancement of deep learning techniques, improved models on the basis of basic methods will provide a solid foundation for more accurate and efficient automatic impact crater detection. In turn, this will promote further research and development in planetary science.

3.4. Deep Learning Applications

Deep learning applications are mainly classified into three categories: semantic segmentation, image classification, and object detection. Table 2 provides a detailed comparison and analysis of these three tasks, including the datasets used for pretraining the models, their respective strengths and weaknesses, and their applications in impact crater detection. The aim is to help new researchers understand the differences between deep learning applications for different tasks so that they can develop deep learning-based CDAs more purposefully.

In summary, deep learning has become a core technical tool for impact crater detection with its powerful automatic feature extraction capability, robustness, and high efficiency. However, the geological environments, surface properties, and diversity of data sources of different celestial bodies lead to differences in the performance of deep learning models on these bodies. To further explore these differences and the causes behind the study, an in-depth analysis of the application of impact crater detection to celestial bodies such as the Moon, Mars, and Mercury is needed. This will help to reveal the applicability and limitations of the models on different planets and provide important references for future model optimization and cross-body transfer learning.

Table 2. Comparative analysis of deep learning applications on different tasks

Task type	Semantic segmentation	Image classification	Object detection
Differences	Semantic segmentation focuses on pixel-level classification, assigning each pixel in the image to a specific object or background.	Image classification only outputs a category label indicating whether or not the image contains an impact crater.	Object detection lies between semantic segmentation and image classification. It outputs category labels and location information (typically bounding boxes) for the objects.
Datasets	PASCAL VOC and MS COCO (Lin et al.[51]; Ali-Dib et al.[32]; Zhang et al.[52]), LVIS, SA-1B (Giannakis et al.[22])	MNIST, CIFAR-10 (DeLatte et al.[16])	COCO (Ali-Dib et al.[32]; Zhang et al., [52]), ImageNet (Yang et al.[53]), MS COCO (Ali-Dib et al. [32]), KITTI, Open Images (Zou et al.[54])
Advantages	Semantic segmentation offers pixel-level precision in impact crater detection, clearly delineating crater boundaries and interior regions. Its advantage lies in capturing detailed spatial shapes and distribution of each crater.	Image classification methods in impact crater detectiondistinguish whether a crater exists in the image. They are mainly applied in more straightforward crater detection tasks. Their advantage is that the model structure is relatively simple, with lower computational costs, enabling fast classification of large-scale images.	Object detection methods in impact crater detection have the advantage of providing both crater category and location information, generating bounding boxes for each detected crater. With the development of object detection algorithms like YOLO and Faster R-CNN, object detection models balance high accuracy and faster processing speed.
Disadvantages	Semantic segmentation models are resource-intensive and require high-quality annotated data during training. Challenges remain in detecting small craters or those with unclear boundaries.	Image classification only provides overall category information for the image, lacking descriptions of crater locations, sizes, and shapes. It is unsuitable for tasks that require precise location and description.	Object detection models have performance limitations in detecting small or overlapping craters, especially in complex terrains and environments with substantial lighting changes. Additionally, they typically require large-scale annotated datasets, especially those with precise bounding box information.
Applications	Segmentation models are widely used in detecting impact craters on different celestial bodies, geomorphological studies, and geological age inference.	Image classification methods are suitable for preliminary screening of high-resolution remote sensing images, such as quickly identifying potential impact crater regions on planetary surface images.	Widely used in real-time planetary exploration, surface navigation, and terrain monitoring tasks.

4. ANALYSIS OF SIMILARITIES AND DIFFERENCES IN IMPACT CRATER DETECTIONON DIFFERENT CELESTIAL BODIES

With the wide application of deep learning in planetary science, various deep learning-based models have been widely used for automatic impact crater detection on a variety of celestial bodies such as the Moon, Mars, and Mercury. However, the performance of the same model on different celestial bodies varies considerably owing to the differences in geological environments, surface material properties, and data resolution. In this section, we combine the research results of Blanco-Rojas et al.[37], Silburt et al.[23], Chen et al.[55], Jia et al.[56], and DeLatte et

al.[16]. We analyze in detail the performance of the CNN-improved-based model and the model on the basis of the U-Net variant on the detection performance on different celestial bodies such as the Moon, Mars, Mercury, and Enceladus. We also assess their generalization ability and their influencing factors for different performance of various models under complex geomorphological conditions.

4.1. Comparison of Model Performance

4.1.1. *Comparison of CNN performance*

To compare the performance of CNN-based improved models in recognizing impact craters on different celestial bodies, we select three celestial bodies, namely the Moon, Mercury, and Enceladus. The Moon's atmosphere-free surface and its clear and widely distributed morphology of impact craters made it an ideal object for studying impact dynamics and secondary crater distribution. Silburt et al.[23] improved the extraction of spatial and semantic features on the basis of an improved CNN method using lunar DEM data in conjunction with a multilevel jump-connect module. The model achieved 92% recall using the test data, and could detect many craters with smaller diameters (15% below the minimum for the original dataset). In addition, the model discriminated well between nested and overlapping crater distributions. However, the complex topographic structure of the lunar surface, especially overlapping regions of impact craters, still caused some interference in the boundary detection of some craters. The study further optimized the detection accuracy by normalizing the image data with cropping, downsampling, and contrast enhancement, also introducing jump-connections to capture multi-scale features.

Mercury's low-gravity environment results in a denser distribution of secondary craters, and its impact crater morphology is similar to that of the Moon to a certain extent. Silburt et al.[23] tested the migration learning performance of a CNN model trained on lunar data by using its migration learning performance on Mercury data. Although the generalization performance of the model on Mercury is slightly lower than that of the Moon, the detection of substantial impact crater boundaries remains more stable. The high-density distribution and complex morphology of Mercury's secondary craters markedly increase the detection difficulty for the model, and it is especially weak in detecting small craters. In addition, because of the difference between Mercury and the Moon in terms of distribution characteristics, the model's accuracy is degraded during the model migration process. The study proposes to improve performance by combining multi-planet data for cross-domain migration training and adapting the multi-scale feature detection module for Mercury's low-gravity environment.

The surface of Enceladus is covered by an icy crust with complex geological activities, such as ice-shell flow and crack formation, resulting in sparse impact craters with indistinct boundaries. Blanco-Rojas et al.[37]proposed a CNN-based multi-level feature extraction model, which utilizes the high-contrast properties of Enceladus's icy surface and substantially improves detection efficiency and accuracy through deep learning. The model achieved approximately 85% detection accuracy on high-resolution image data of Enceladus and especially excelled in the detection of small craters (less than 10 km in diameter). However, because of the geologic activity of the dynamic ice crust and sediment masking, some of the secondary pits have high boundary ambiguity, which affects the detection. The study employs data enhancement techniques to optimize high-contrast imagery while incorporating a template matching algorithm to improve boundary segmentation accuracy and address these challenges.

The performance of CNN-based models on the Moon, Mercury, and Enceladus reveals the differences in the properties of impact crater detection on different celestial bodies and their impact on the models (summarized in Table 3). By adapting to the geological and data properties of other celestial bodies, the models achieve high detection efficiency while at the same time exposing the deficiencies in the cross-domain generalization capability of the CNN-based deep learning models. These studies provide important directions for future crater detection improvements on other celestial bodies.

4.1.2. *Comparison of U-net performance*

To compare the performance of U-Net variant-based models for recognizing impact craters on different celestial bodies, we look at Mars and the Moon. Impact craters on Mars are of great importance in studying geological evolution and depositional environments, especially in regions where regolith deposition is more active. The studies of Chen et al.[55] and DeLatte et al.[16] explored the application of the U-Net improved model for Martian impact crater detection. The Martian Crater U-Net (MC-UNet) model proposed by Chen et al[55]. achieves efficient detection of impact craters of 2 to 32 km in diameter by increasing the network depth and embedding an attention mechanism to focus on the semantic segmentation task in infrared images from the Thermal Emission Imaging System (THEMIS). By contrast, DeLatte et al.[16] designed a lightweight network on the basis of Crater U-Net, which can better adapt to the fast processing of large-scale image data. Regarding detection performance, MC-UNet achieved an F_1-score of 0.8355 on the test set, demonstrating superior precision and recall, being particularly reliable in the detection of medium-sized (diameter > 5 km) impact craters. However, the model's detection performance deteriorates in areas with a large amount of regolith deposition. Crater U-Net achieves 65%–76% matching accuracy in pixel-level tests, and although it detects quickly, it needs further optimization for detection in areas with dense secondary craters.

The lunar surface, with no atmosphere, clear morphology, and dense distribution of impact craters, is an ideal celestial body for studying impact dynamics. Jia et al. [56]

Table 3. Summary of the performance of improved CNN-based model impact crater detection on the Moon, Mercury, and Enceladus

Celestial body	Data characteristics	Model improvements	Detection performance	Main challenges	Specific preprocessing requirements
Moon[23]	No atmosphere, clear crater morphology	Skip connection to capture multi-scale features	Recall rate 92%	Nested crater complexity, boundary interference from overlapping craters	DEM data augmentation, boundary optimization
Mercury[23]	Low gravity, dense secondary craters	Generalization testing, lunar transfer learning	Lower accuracy than the Moon	Data distribution differences, complex secondary crater morphology	Cross-domain learning, feature optimization
Enceladus[37]	Ice shell coverage, high contrast	Multilevel feature extraction	Accuracy is around 85%	Dynamic changes in the ice shell and blurry boundaries of secondary craters	High contrast optimization and template matching

proposed Need-Attention-Aware U-Net (NAU-Net) on the basis of the U-Net++ architecture, incorporating nested dense connectivity and an attention mechanism to substantially improve the ability of the model to detect overlapping craters and complex boundary regions. In detection performance, NAU-Net achieves a recall of 0.791 and an accuracy of 0.856 on monthly DEMs, which is superior to the traditional U-Net model. In particular, NAU-Net shows strong adaptability in the tasks of secondary crater detection with a diameter of less than 1 km and segmentation of regions with fuzzy boundaries. To improve the detection accuracy, the study adopts high-precision calibration of DEM data for standardization and combines the template matching algorithm for post-processing to optimize the boundary positioning and size correction further.

The above analysis demonstrates the performance difference of the U-Net variant-based models in Mars and Moon impact crater detection. Table 4 visualizes the advantages and disadvantages of the models as well as the applicable scenarios. These studies provide technical support for impact crater detection of different celestial bodies and point out the optimization direction for future cross-domain applications.

4.2. Key Factors Influencing Model Performance

The performance of impact crater detection models on celestial bodies such as the Moon, Mars, Mercury, and Enceladus is influenced by a combination of celestial body properties, data preprocessing requirements, and model architecture design. The properties of the celestial bodies themselves determine the preservation status and morphological characteristics of impact craters. For example, with no atmosphere and weak geological activity, the Moon has clear and long-term stable impact crater boundaries, providing ideal detection conditions for the model. At the same time, Mars shows wind-sand depositional effects and sedimentary cover that make the edges of many craters indistinct, rendering detection more difficult. Mercury, with its lower gravity, leads to a dense distribution and complex morphology of secondary craters, which puts higher demands on the generalization ability of the model. Enceladus's ice-shell-covered environment, however, creates unique detection challenges owing to the dynamics of the ice mass and the high-contrast surface properties.

In addition, there are notable differences in the data preprocessing needs of different celestial bodies. For example, lunar impact crater detection relies mainly on DEM data, which have higher resolution and are not affected by ambient light. In contrast, Mars detection missions usually rely on multispectral infrared images (e.g., THEMIS data), which require spectral separation and contrast enhancement to fit the modeling needs. For Mercury, the data distribution is similar to that of the Moon, but the secondary crater detection of its small craters is more difficult because of the different gravity environments. However, Enceladus requires specific contrast enhancement and template matching algorithms on the basis of its high-contrast characteristics to cope with indistinct boundaries on icy surfaces.

The architectural design of a model inevitably impacts performance. The introduction of an attention mech-

Table 4. Summary of the performance of U-Net variant-based model impact crater detectionon Mars and the Moon

Celestial body	Model	Data type	F_1-score	Recall	Accuracy	Advantages	Challenges
Mars[55]	MC-UNet	THEMIS infrared images	0.8355	0.791	0.850	Accurate detection of medium-sized impact craters, precise boundary detection for large craters interference from overlapping craters	Performance degradation in sand and dust deposition areas
Mars[16]	Crater U-Net	THEMIS infrared images	0.650–0.760	–	–	Fast detection of secondary craters, lightweight network suitable for big data processing	Need for more detection accuracy in secondary crater-dense areas
Moon[56]	NAU-Net	DEM data	–	0.791	0.856	Strong detection capability for overlapping craters and blurred boundary areas	High data resolution and relatively high model complexity

anism enhances the model's ability to focus on critical regions (e.g., crater edges and interior details), while a multiscale feature extraction module strongly affects the handling of sedimentary cover and complex crater morphology. These techniques have yielded promising results in impact crater detection on Mars and the Moon and have shown some adaptability in detection missions on Enceladus and Mercury. Table 5 provides a comparative summary of the key factors affecting model performance.

4.3. Quantitative Comparison of the Performance of Different Models for Impact Crater Detection on the Surfaces of Various Celestial Bodies

Here, we quantitatively compare the performance of different deep learning models for impact crater detection on the surface of the Moon, Mars, and other celestial bodies. These models include traditional CNN, U-Net variants, and Faster R-CNN, which are applied to different datasets such as Lunar Reconnaissance Orbiter Camera (LROC), Thermal Emission Imaging System (THEMIS), and High Resolution Imaging Science Experiment (HiRISE). Differences in the morphology, size, and distribution of impact craters, as well as planetary surface environments, affect the performance of the models, so we evaluate the performance of different models on these datasets.

Table 6 shows the performance of different deep learning models in the task of impact crater detection on the surface of the Moon, Mars, and other celestial bodies. The table lists the precision, recall, and F_1-scores of each model on different datasets and provides the corresponding dataset source and resolution information to clearly show the differences in the performance of each model on different planetary datasets and better evaluate the effectiveness of each method.

5. EXISTING CHALLENGES AND FUTURE RESEARCH DIRECTIONS

5.1. Existing Challenges

In the process of developing automatic detection of impact craters on planetary surfaces, researchers have faced many challenges, especially in terms of data scarcity, model generalization ability, algorithm efficiency, complexity of impact crater features, and data acquisition and processing. Here, we introduce the specific problems one by one and discuss possible solutions.

5.1.1. *Data scarcity*

Impact crater detection on planetary surfaces is a typical data-intensive task, but the existing impact crater datasets are clearly insufficient in terms of quantity and diversity. Currently, impact crater datasets are mainly derived from satellite missions, such as the LRO and Kaguya, which collect a large number of images of impact craters, particularly of large and apparent craters. However, most of the labeled data in these datasets are limited to large impact craters that are relatively clear, while labeled data are scarce for smaller, blurred, or shadowed impact crater images. Consequently, the question of how to construct effective deep-learning models in the presence of data scarcity is a major challenge in current research.

There are many solutions given in recently published scientific literature. For example, Giannakis et al.[22] proposed the use of the Segment Anything Model (SAM) to solve the problem of data scarcity, which enhances the model's learning ability on a small amount of labeled data through a weakly supervised learning strategy. This approach improves the detection accuracy of small impact craters on the surface of celestial bodies by pretraining with large-scale unlabeled data.

To further address the challenge of insufficient data, Yang and Cai[3] employed a migration learning technique to enhance the robustness of the impact crater detection model. Migration learning is able to migrate models already trained on other celestial bodies to another celestial body for impact crater detection, effectively alleviating the dilemma of scarce training data. The data enhancement method, however, improves the generalization ability of the model by synthesizing more variant samples through operations such as rotating, scaling, and clipping.

To overcome the challenges posed by data scarcity and advance the field of impact crater detection, it is crucial to use publicly available and standardized impact crater datasets for model benchmarking. Such datasets currently used for impact crater detection, including LROC, HiRISE, and THEMIS are shown in Table 7, and pro-

Table 5. Comparative summary of key factors affecting model performance

Celestial body	Planetary characteristics	Data type	Preprocessing requirements	Model requirements
Moon[23]	Clear boundaries, no atmosphere, no sediment cover	DEM data	Resolution adjustment, contrast enhancement	Multi-scale feature extraction
Mars[16, 55]	Fuzzy boundaries, active sand, and dust deposition	THEMIS infrared data	Multispectral separation, illumination correction, noise reduction	Attention mechanism to enhance the capture of fuzzy areas
Mercury[56]	Dense secondary craters and clear boundaries	DEM data	A model transfer on the basis of Moon data supplements secondary crater training.	Generalization ability optimization
Enceladus[37]	Icy shell coverage, high contrast, dynamic boundary changes	High-resolution imagery data	High contrast optimization and template matching	Dynamic adaptation to icy shell, feature extraction optimization

Table 6. Quantitative comparison of the performance of different models in impact crater detection across the surfaces of various celestial bodies

Source	Celestial body	Model	Dataset	Resolution/ (m/pixel)	Precision/ (%)	Recall/ (%)	F_1-score/ (%)
Xiong et al.[57]	Moon	Lunar Topographic Knowledge Attention U-Net (LTKAU-net)	DEM (D > 5 km)	59	56.00	89.00	68.00
Zhong et al.[58]	Moon	Faster R-CNN + Super-Resolution Network (SR-Net)	DEM (D > 1 km)	59	76.00	81.20	78.50
Mohite et al.[59]	Moon	Residual U-Net34/ 50 (ResUNet-34/50)	DEM	118	83.67	77.22	80.61
Nan et al.[60]	Moon	You Only Look Once version 8-Lunar Crater Network (YOLOv8-LCNET)	Digital Orthophoto Map (DOM) mosaics	0.86 and 0.6	87.70	84.30	85.90
Zhang et al.[52]	Moon	Center-based Object Detection Network (CenterNet)	LRO Wide Angle Camera (WAC) ortho-image	100	78.27	73.66	75.96
Yang et al.[61]	Moon	CenterNet	DEM (Kaguya and LRO)	59	80.10	68.40	73.70
Liu et al.[41]	Moon	Faster R-CNN + Region of Interest Align (RoI_Align)	Kaguya TC morning (D > 200 m)	10	90.19	96.33	93.34
Zou et al.[54]	Moon	Faster R-CNN + RoI_Align	A high-resolution digital orthophoto image of the CE-5 landing site	1.5	69.00	90.00	78.04
Ye et al.[62]	Mars	Random Sampling and Local Feature Aggregation Network (RandlaNet) with multi-scale sampling	DEM (ESA Mars Express)	50	91.70	87.50	89.50
Yu et al.[63]	Mars	YOLOv9 + Atrous Spatial Pyramid Pooling (ASPP) +Deformable Convolutional Network (DCN)+ Cross Stage Partial Efficient Layer Aggregation Network (CSPELAN)	Detection of Automatic Crater Dataset (DACD)	25	85.42	80.85	82.72
Lee[64]	Mars	CNN	Digital Terrain Model (DTM)	200	89.00	43.00	59.00
Pedrosa et al.[65]	Mars	Morphological Image Processing (MIP) + Fast Fourier transform (FFT)	THEMIS	100	92.23	92.81	92.52
Jin et al.[66]	Mars	Adaptive Boosting (Adaboosting)	High Resolution Stereo Camera (HRSC)	12.5	85.00	85.20	85.10
Emmanuel et al.[67]	Earth	Random Forest	Shuttle Radar Topography Mission (SRTM) DEM	30	74.10	83.30	78.57
Blanco-Rojas et al.[37]	Enceladus	Deep Convolutional Neural Network for Semantic Image Segmentation, Version 3 Plus (DeepLabV3+)	Cassini Imaging Science Subsystem (ISS)	100	83.00	–	–

vide rich impact crater image data on different celestial bodies to help model training and evaluation.

When creating publicly available, annotated datasets of impact craters, they should include craters identified manually by experts as well as craters identified using CDAs. Such annotated datasets of impact craters, created for various celestial bodies in recent years, are shown in Table 8 and Table 9 for the benefit of new researchers to learn from.

5.1.2. *Model generalization ability*

With the increasing application of deep learning methods in impact crater detection, the generalization ability of the model becomes another key issue. The shapes and features of planetary impact craters are diverse and the impact craters in different regions have different scales, depths, shapes, and lighting conditions. Existing models often perform well in specific datasets or environments, but tend to substantially degrade in performance with different illumination conditions, resolutions, and crater types. Improving the adaptability and accuracy of the model in different scenarios has become a key issue in further enhancing the accuracy of impact crater detection.

Table 7. Standard datasets and access links (Data from various NASA and ESA missions)

Celestial Body	Dataset	Open access	Access link
Moon	LROC	Accessible	https://ode.rsl.wustl.edu/odeholdings/Moon_holdings.html
Mars	HiRISE	Accessible	https://www.uahirise.org/
Mars	THEMIS	Accessible	https://pds.nasa.gov/
Mercury	MESSENGER	Accessible	https://pds.nasa.gov/
Earth	SRTM DEM	Accessible	https://www.nasa.gov/stem-content/earth-observing-system-data-and-information-system/
Titan	ISS	Accessible	https://pds.nasa.gov/
Enceladus	ISS	Accessible	https://pds.nasa.gov/
Venus	Magellan	Accessible	https://pds.nasa.gov/

Table 8. List of manually identified crater databases

Source	Celestial body	Spacecraft	Dataset	Resolution	Impact crater database
Head et al.[68]	Moon	LRO- Lunar Orbiter Laser Altimeter (LOLA)	DTM/DEM	64 pixels/(°)	5 185 impact craters with diameter $D \geqslant 20$ km
Salamunićcar et al.[69]	Moon	LRO-LOLA, Selene, and the Martian	DEM	512 pixels/(°)	60 645 impact craters with diameter $D \geqslant 8$ km and 132 843 with diameter $D \geqslant 2$ km
Povilaitis et al. [70]	Moon	LROC-WAC ± (78–90)°N	Global images and DTM	303 pixels/(°)	22 746 impact craters with diameter D between 5–20 km
Robbins[71]	Moon	LROC-WAC, LOLA gridded and merged Terrain Camera (TC) DTM, LOLA mosaic, and TC DTM + LOLA mosaic	Multi-source dataset	LROC's WAC approximately 100 m/pixel, LOLA gridded approximately 433 pixels/(°), merged TC DTM approximately 1010 pixels/(°), LOLA approximately 3 030 to 6 060 pixels/(°)	~1.3 million impact craters with diameter $D \geqslant 1$ km, ~83 000 impact craters with diameter $D \geqslant 5$ km, 6 972 impact craters with diameter $D \geqslant 20$ km
Barlow[72]	Mars	Viking 1 spacecraft	Multi-source dataset	131 pixels/(°)	25 826 impact craters with diameter $D \geqslant 8$ km
Robbins and Hynek[7]	Mars	Mars Reconnaissance Orbiter (MRO)	DEM and multiple data sources	303 pixels/(°)	384 343 impact craters with diameter $D \geqslant 1$ km
Salamunićcar et al.[69]	Mars	Various data sources	DEM and image data	512 pixels/(°)	57 633 manually compiled impact craters
Kinczyk et al. [73]	Mercury	MESSENGER	Mercury image data	66 332, 665 655 m/pixel	All impact craters with diameter $D \geqslant 40$ km on Mercury
Earth Impact Database	Earth	Multiple Earth data sources	Global Earth impact crater images and geological data	Various resolutions	It contains globally known Earth impact craters, widely used for geological and paleoclimate research.
USGS Global Impact Crater Database	Earth	United States Geological Survey (USGS)	Earth images and geological data	Various resolutions	Contains impact crater information for Earth, used for studying major historical impact events.
Lorenz et al.[74]	Titan	Cassini RADAR	Titan SAR image data	Various resolutions	Includes three confirmed impact craters (Menrva, Sinlap, Ksa) and several candidate impact structures, with diameters ranging from 4 km to 400 km.

To solve the problem of insufficient generalization ability of the model, Jia et al.[19] used the SplitAttention network combined with self-calibrated convolution to capture the complex features of the lunar surface. The advantage of this method is that the model can adaptively adjust the weights of the convolution kernel in multiple environments, which improves the generalization ability to different scenarios.

In addition to the improvement of model architecture, Jia et al.[83] proposed the Attention-Enhanced Transformer U-Net Plus (AE-TransUNet+) model, which combines the Transformer and U-Net architectures to further

Table 9. List of automated crater databases

Source	Celestial body	Spacecraft	Dataset	Resolution	Impact crater database
Salamunićcar et al.[75]	Moon	LRO-LOLA, GLD100 LRO WAC	DEM and orbital images	DEM: 512 pixels/(°), orbital images: 303.2340 pixels/(°)	78287 impact craters with diameter $D \geqslant 8$ km
Silburt et al.[23]	Moon	LRO and Kaguya	DEM	512 pixels/(°)	361 new impact craters with diameter $D < 5$ km
Yang et al.[76]	Moon	Chang'e 1 and 2	DOM and DEM data	DOM resolution: 120 m and 7 m, DEM resolution: 500 m and 7 m	18 996 impact craters with diameter $D \geqslant 8$ km and 117240 with diameter $D \geqslant 1$ km
Cadogan[77]	Moon	LROC-NAC	Low-resolution DTM input and grayscale images	0.5 m/pixel	Over 300 000 impact craters with diameter $D \geqslant 2.5$ m
Jia et al. [56]	Moon	Chang'e 1, SELENE Lunar Digital Elevation Model (SLDEM), and Kaguya merged DEM	SLDEM and DOM	59 m/pixel and 120 m/pixel	157389 impact craters with diameter D from 0.6 to 860 km
Lin et al.[51]	Moon	LRO-LOLA and Kaguya (SELENE) TC	DEM	512 pixels/(°)	31606 impact craters with diameter D between 1 and 20 km
Tewari et al.[78]	Moon	LRO-LOLA, Selene TC	SLDEM	100 m/pixel	22746 impact craters with diameter D between 5 and 20 km
Liu et al.[41]	Moon	Chang'e 5, Kaguya TC	Morning map	7.403 m/pixel	187101 impact craters with diameter $D \geqslant 200$ m
Stepinski et al.[79]	Mars	Mars Orbiter Laser Altimeter (MOLA)	DEM	128 pixels/(°)	Multi-scale Mars impact crater database
Lagain et al.[80]	Mars	Various (including CTX global images)	High-resolution remote sensing images	Various resolutions	Impact craters larger than 1 km, including 8445 LERS craters, 24530 partially buried craters, 55309 secondary craters, 288155 standard craters, and 39000 secondary craters linked to 108 primary craters
Yang and Cai[3]	Mars	Thermal Infrared Imaging System	Mars Digital Crater Database (MDCD)	256 pixels/(°)	Approximately 12000 impact craters, with diameters ranging from 6 pixels to 250 pixels; most craters have diameters smaller than 50 pixels, and about 3 000 craters have diameters around 10 pixels, with fewer than 1% having diameters over 200 pixels.
Herrick et al.[24]	Mercury	Mercury Dual Imaging System (MDIS) v9, Laser Altimeter, Stereo Imaging Data	Panchromatic mosaic, mask, Topography	5 km data resolution	31600 impact craters larger than 5 km, including 17000 craters larger than 10 km, excluding obvious secondary craters. Morphological features recorded included volcanic fills, central structures, degradation states, halos, etc.
Lyapidevskaya and Gusiakov[81]	Earth	Various data sources	EDEIS (Earth Impact Database)	Various resolutions	1082 meteorite craters: 206 fully confirmed, 186 highly probable, 501 probable, 75 suspected, and 114 excluded
Neish and Lorenz[82]	Titan	Cassini radar	Titan radar image data	Various resolutions	About 50 impact craters: diameters greater than 3 km, confirmed and potential impact craters, including Selk and Afekan

enhance the adaptability of impact crater detection across different environments. The Transformer structure can focus on key features through the self-attention mechanism, which enables the model to accurately recognize impact craters in complex and noisy environments.

For the extension of domain adaptation methods, some recent studies have explored bridging the differences between impact crater images from different objects using synthetic dataset enhancement techniques, i.e., generating synthetic image data that simulate impact crater fea-

tures from different objects to enhance the generalization ability of the model. Wang et al.[38] proposed a novel active machine learning approach by combining Two-Dimensional (2D) images and Three-Dimensional (3D) data from DEM to collect training samples semi-automatically. The method first co-aligns the image and DEM datasets, then actively requests annotations on 2D features derived from the image and inputs 3D features derived from the DEM during the training process to update the training pool and retrain the model. This process can be performed multiple times to obtain a sufficient number of training samples with good quality, which in turn improves the performance of the classifier and applies it to automatic impact crater detection in other regions. The test results of the final trained model on the lunar and Martian datasets show that the True Detection Rate (TDR) and False Detection Rate (FDR) of the lunar dataset are 93.63% and 10.74%, respectively, while those of the Martian dataset are 92.27% and 3.83%, respectively. TDR refers to the proportion of true positive detections (correctly identified craters or features) out of all the actual positive instances in the dataset. FDR refers to the proportion of false positives (incorrectly identified craters or features) out of all the instances that were predicted as positive by the model. Both are good performances, demonstrating that the synthetic dataset enhancement technique is able to effectively bridge the differences between the images of impact craters from different celestial bodies and to enhance the generalization ability of the model.

Through domain migration learning, a model that has been trained on one celestial body can be applied to another celestial body, thus improving the performance of the model on different celestial surfaces, by means of pretrained models, fine-tuning, feature sharing, or multi-task learning. Silburt et al.[23] applied a model on the basis of a CNN model, pretrained on lunar data, to Mercury's dataset effectively. It performed well, identifying most of the impact craters in all DEM data for Mercury, suggesting that the model can be effectively appliedto other celestial bodies with DEM data. This demonstrates that the strategy of domain migration between planetary datasets improves the fitness of a model in a variety of planetary surface environments.

5.1.3. *Algorithm efficiency*

The automated detection of impact craters requires not only high accuracy but also high efficiency. For large-scale planetary surface data, such as LRO images, the processing speed and real-time performance become difficult for impact crater detection. Especially in application scenarios that require fast analysis and real-time feedback, deep learning models often require a lot of computational resources and time. Complex deep learning models, such as CNNs and Transformer networks, usually require a large amount of computational and storage resources, which requires improving accuracy while minimizing computational complexity, maintaining fast processing speed and low resource consumption.

As deep learning models become more and more complex, the task of impact crater detection causes great pressure on computational resources, especially in tasks with high real-time requirements. For example, the Efficient Lunar Crater Detection (ELCD) model proposed by Fan et al.[84] employs a multi-scale feature fusion and attention mechanism, which allows the algorithm to considerably reduce the computational complexity while guaranteeing higher accuracy. The model is designed to process large-scale DEM data for efficient detection of impact craters while ensuring real-time performance. As an alternate solution, DeLatte et al.[16] proposed a CNN-based framework for impact crater detection in response to the real-time problem of the algorithm, which further reduces the computational burden through the embedded feature selection and boosting technique. This method is capable of accomplishing accurate detection of impact craters in a shorter time while maintaining a low FP rate when processing large-scale images of planetary surfaces.

5.1.4. *Complexity of impact crater features*

Planetary impact craters have different morphologies, with different scales, depths, shapes, and distributions, making their representation in images very complex. In particular, small impact craters are often blurred because of low resolution or affected by factors such as lighting, shadows, and dust. This makes them difficult to recognize using traditional image processing methods. Most deep learning models tend to perform poorly in detecting these small impact craters because they rely on precise edges, contrast, and structural information, which are often insignificant visual features.

Another consideration is that the spatial heterogeneity of impact crater features means that impact craters in different regions of a celestial body may have marked differences in size, shape, and distribution, causing additional complexity for model training and prediction. For example, the impact crater densities and morphological features in the polar and equatorial regions of the Moon differ notably. Ensuring that the model can accurately detect different types of impact craters across geographic regions and scales is an issue that should not be ignored.

The shape, size, distribution, and other features of impact craters pose a great challenge to automatic detection. In particular, small impact craters and fuzzy impact craters usually make it difficult to extract effective features directly from images owing to insufficient resolution or poor image quality. Fairweather et al.[20] proposed a method, capable of handling impact craters at different scales and accurately recognizing small and indistinct craters, to automatically calibrate lunar impact craters using LRO-Narrow Angle Camera (LRO-NAC) images. However, despite the high detection accuracy of the method, it still faces the problem of distinguishing small impact craters in low-contrast environments. To solve this problem, Emami et al.[18] introduced the combination of

unsupervised learning and CNNs and proposed a novel framework for impact crater detection. The framework deals with blurred images of impact craters on the lunar surface by convex packet grouping of the images. This method is able to effectively recognize small impact craters even without labeled data. In addition, Hashimoto et al.[85] used a deep learning method on the basis of grid segmentation to detect impact craters and proposed processing low-resolution images using an improved CNN. In this way, the method improves the detection accuracy of blurred regions and low-contrast, small-impact craters.

5.1.5. *Data acquisition and processing*

Satellite missions such as LRO and Kaguya have provided a large amount of valuable image data, but there are many difficulties in processing these data. For example, images of impact craters on the lunar surface are often noisy and of low resolution, and there are substantial differences in image quality and resolution between different sensors, which makes it challenging to ensure the uniformity and consistency of the data. In addition, because the labeling of lunar impact craters is exceptionally tedious, it is often necessary to rely on experts to manually label the data, and the manual labeling of data faces the problem of time, cost, and accuracy. Therefore, the problem of efficiently processing and labeling these data, especially for practical training without labeled data, still requires an urgent solution.

To address this problem, Fairweather et al.[36] discussed how to integrate the LRO-NAC and Kaguya TC image datasets to improve the accuracy of impact crater detection by combining automated and manual labeling. The preprocessing of image data (e.g., denoising, image alignment) becomes a major challenge in this process. Ghilardi[86] proposed a deep learning model on the basis of semantic segmentation for automated calibration of impact craters when processing low-quality images. This method accurately calibrates the impact crater regions in images using a semantic segmentation technique, which greatly reduces the workload of traditional manual labeling. Additionally, Fan et al.[84] proposed a framework for lunar impact crater detection on the basis of multiscale feature fusion, which showed good adaptability in processing image data with different resolutions and noise interference.

Although there are some practical solutions, how to deal with large-scale, multisource heterogeneous planetary image data is still an important direction for future research.

5.2. Future Research Directions

With the wide application of deep learning techniques in crater detection, future research should further enhance the generalization capability of the models, strengthen data fusion techniques, and explore a wider range of scientific application directions to cope with the complexity and diversified needs in diverse celestial environments. To that end, we offer some suggestions here for future research directions.

First, multimodal data fusion is a key strategy to improve model detection accuracy and adaptability. Combining multisource data such as DEM, multispectral images, infrared images, and radar data, the model can be provided with richer feature information. For example, in the wind–sand deposition regions of Mars, the superposition processing of hyperspectral data with infrared images can effectively make up for the interference of the depositional mask on the detection of impact crater boundaries. On the ice-shell surface of Enceladus, the segmentation accuracy of indistinct crater boundaries can be improved by combining the high-contrast images with the ice-shell dynamic model. Multimodal data fusion not only enhances the ability of the model to capture detailed features but also provides technical support for cross-domain studies in multiplanet environments.

In current impact crater detection tasks, SSL with physics-informed deep learning provides an important technological way to improve the performance and adaptability of models. SSL, as an innovative learning paradigm, can utilize a large amount of unlabeled data for pretraining in the absence of labeled data. Through this pretraining process, the model is able to learn rich feature representations and optimize the learning process through a self-supervised mechanism, effectively improving adaptability on different datasets, especially in the case of data scarcity. Specifically, through SSL, the model is able to automatically generate labeling information or construct learning objectives and conduct deep feature learning on this basis. Therefore, in impact crater detection, the use of SSL can effectively extend the training dataset of the model and improve its generalization ability to unseen images, especially in planetary datasets for which it is difficult to obtain a large amount of labeled data.

Physics-informed deep learning is another technique which combines the advantages of physical modeling and deep learning to further improve the accuracy and reliability of impact crater detection. In the impact crater detection task, physics-informed deep learning can help the model better understand and capture the features of impact craters by incorporating the physical properties of the planetary surface (such as albedo, thermal properties, and surface structure) into the deep learning framework. By introducing these physical models, deep learning networks are able to constrain the output of the model to make more accurate predictions with physical consistency. For example, by using surface reflectance or thermal radiation properties as input features, physics-informed deep learning can substantially improve the accuracy of impact crater detection in complex environments such as different lighting conditions or environments.

Terrain data, such as DEMs, can provide 3D topographic features of impact craters, further optimizing the model's detection of impact crater depth and shape. Through multimodal learning, the model is able to consider both the visual information of the image and the geometric information of the terrain, consequently perform-

ing more accurately and robustly in the task of impact crater detection for multiple celestial objects. Combining these data, the deep learning model is not only able to recognize impact craters from a single viewpoint but also synthesize various types of information to improve the adaptability to diverse environments and complex situations.

In summary, SSL and physics-informed deep learning provide new ideas and technological breakthroughs for impact crater detection, especially in the case of data scarcity and diverse data sources, while multimodal data fusion further enhances the accuracy and generalization ability of the model. These techniques will play an important role in future research on planetary impact crater detection.

A second possible direction uses domain adaptation and cross-body migration learning to provide a means to improve the cross-domain generalization ability of models. There are clear differences in the geologic properties and data distributions of different planets, such as the densities of secondary craters on Mercury versus the Moon, and the clarity of the boundaries of impact craters on Enceladus and Mars. These differences often pose challenges to model performance. By introducing unsupervised domain adaptation techniques, the impact of data distribution differences can be effectively reduced; combining the shared characteristics of multiplanet data can optimize the model's detection capability. In addition, the cross-body migration learning technique can utilize existing high-quality data to extend the model to data-scarce celestial bodies, further improving the efficiency of deep space exploration missions.

The effective use of high-resolution observational data will improve the efficiency of impact crater detection. With high-resolution remotely sensed data available, models can more accurately capture detailed features of impact crater boundaries. For example, high-resolution radar data allow precise detection of impact craters on icy objects and in sediment-covered regions, while in the atmosphere-free environments of the Moon and Mercury, smaller secondary craters can be detected using ultrahigh-resolution optical imagery. Future research could focus on developing automated preprocessing processes for high-resolution data and designing effective data fusion strategies to maximize their scientific value.

Finally, deep learning-based impact crater detection techniques can be extended to a broader range of scientific applications, including geological evolution analysis and impact crater age estimation. For example, recognizing the morphology and distribution pattern of impact craters can not only improve the accuracy of planetary chronology but also reconstruct the geological evolution history of celestial bodies. Additionally, combining the geometric features of impact craters with hyperspectral data can be used to analyze the sediment and tectonic properties of craters, revealing the dynamic processes of planetary material cycling and environmental changes. The expansion of these applications will further highlight the great potential of deep learning in planetary science research.

In addition, to facilitate subsequent research, we summarize the databases of impact craters on the surfaces of the Moon, Mars, and Mercury, as shown in Table 8, which were manually identified and compiled by experts in planetary sciences to assist new researchers. Table 9 shows databases of new impact craters identified using automated CDA techniques. This table can provide a valuable resource for new researchers to create new impact crater databases.

6. SUMMARY AND OUTLOOK

In this paper, we summarized the application of deep learning to the detection of impact craters on different celestial bodies, and analyzed the differences in the features of planets such as the Moon, Mars, and Earth, and their impact on model performance. The straightforward impact crater morphology of the Moon can be preserved for an extended period, making it suitable for model training. By contrast, the boundaries of impact craters on Mars, Enceladus, and Mercury are more ambiguous owing to processes such as wind-sand deposition and ice-shell dynamics, which make detection more difficult. The differences in the morphology and preservation status of impact craters on different celestial bodies also have different impacts on the adaptability and accuracy of the model.

The deep learning models we have examined, on the basis of CNN improvement and U-Net variants, have made good progress in impact crater detection, but the performance in cross-body migration and complex geological environments still needs to be improved. Future research can improve the generalization ability and detection accuracy of the models through techniques such as multimodal data fusion and cross-body migration learning. Combining multisource data such as DEM, spectral images, and radar data can also provide richer features for the model and help solve the problem of variability among different planets.

Applying deep learning technology can also extend beyond impact crater detection. It can also be expanded to the analysis of planetary evolution, estimating the age of impact craters, and other fields, providing more scientific data for deep space exploration. With the continuing advancement of technology, deep learning will play an increasingly important role in planetary science and provide more substantial technical support for future deep space exploration.

ACKNOWLEDGEMENTS

This work was funded by the National Natural Science Foundation of China (12363009 and 12103020), Natural Science Foundation of Jiangxi Province (20224BAB211011), Youth Talent Project of Science and Technology Plan of Ganzhou (2022CXRC9191 and 2023CYZ26970), and Jiangxi Province Graduate Innova-

tion Special Funds Project (YC2024-S529 and YC2023-S672).

AUTHOR CONTRIBUTIONS

Xu Zhang contributed to the conceptualization of the study, developed the methodology, conducted the literature review, and was responsible for drafting the original manuscript. Jialong Lai contributed research support and reviewed the manuscript critically. Feifei Cui contributed to the methodology development and assisted in the overall research process. Chunyu Ding provided feedback on the methodology and played a critical role in the data analysis process. Zhicheng Zhong assisted with the literature collection and provided valuable input during the manuscript drafting process. All authors read and approved the final manuscript.

DECLARATION OF INTERESTS

The authors declare no competing interests.

REFERENCES

[1] Chinmayee, C., Vijay, K. J. 2024. A review on deep learning-based automated lunar crater detection. *Earth Science Informatics*, **1**(17): 3863−3898.

[2] Yang, Y. Z., Liu, Y. 2022. The Chang'e-4 rover detected impact remnants rich in carbonaceous chondrite on the far side of the Moon. *Reviews of Geophysics and Planetary Physics*, **53**(2): 233−235. (in Chinese)

[3] Yang, S. J., Cai, Z. C. 2021. High-resolution feature pyramid network for automatic crater detection on Mars. *IEEE Transactions on Geoscience and Remote Sensing*, **60** (7): 1−12.

[4] Yang, M., Zhang, B. Y., Yan, X. Y., et al. 2024. Development of the fine lunar gravity field modeling with digital elevation model. *Reviews of Geophysics and Planetary Physics*, **55**(5): 513−523. (in Chinese)

[5] Agarwal, N., Haridas, A., Khanna, N., et al. 2019. Study of morphology and degradation of lunar craters using Chandrayaan–1 data. *Planetary and Space Science*, **167**: 42−53.

[6] Allen, C. C. 1975. Central peaks in lunar craters. *Moon*, **12** (4): 463−474.

[7] Robbins, S. J., Hynek, B. M. 2012. A new global database of Mars impact craters ⩾1 km: 1. Database creation, properties, and parameters. *Journal of Geophysical Research: Planets*, **117**: E05004.

[8] Robbins, S. J., Antonenko, I., Kirchoff, M. R., et al. 2014. The variability of crater identification among expert and community crater analysts. *Icarus*, **234**: 109−131.

[9] Greeley, R., Gault, D. E. 1970. Precision size-frequency distributions of craters for 12 selected areas of the lunar surface. *Moon*, **2**(1): 1077.

[10] Kirchoff, M., Sherman, K., Chapman, C. 2011. Examining lunar impactor population evolution: Additional results from crater distributions on diverse terrains. In Proceedings of EPSC-DPS Joint Meeting.

[11] Ding, W., Stepinski, T. F., Bandeira, L., et al. 2010. Automatic detection of craters in planetary images: An embedded framework using feature selection and boosting. In Proceedings of the 19th ACM International Conference on Information and Knowledge Management.

[12] Burl, M. C. 2001. Automated detection of craters and other geological features. In Proceedings of 6th International Symposium on Artificial Intelligence, Robotics and Automation in Space.

[13] Li, B., Ling, Z. C., Zhang, J., et al. 2015. Automatic detection and boundary extraction of lunar craters based on LOLA DEM data. *Earth Moon Planets*, **115**: 59−69.

[14] Boukercha, A., Al-Tameemi, A., Grumpe, A., et al. 2014. Automatic crater recognition using machine learning with different features and their combination. In Proceedings of 45th Annual Lunar and Planetary Science Conference.

[15] Chen, D., Hu, F., Zhang, L. Q., et al. 2024. Impact crater recognition methods: A review. *Science China Earth Sciences*, **67**(6): 1719−1742.

[16] DeLatte, D. M., Crites, S. T., Guttenberg, N., et al. 2019. Automated crater detection algorithms from a machine learning perspective in the convolutional neural network era. *Advances in Space Research*, **64**(8): 1615−1628.

[17] Cohen, J. P., Lo, H. Z., Lu, T., et al. 2016. Crater detection via convolutional neural networks. *arXiv: 1601.00978*.

[18] Emami, E., Ahmad, T., Bebis, G., et al. 2019. Crater detection using unsupervised algorithms and convolutional neural networks. *IEEE Transactions on Geoscience and Remote Sensing*, **57**(8): 5373−5383.

[19] Jia, Y. T., Liu, L., Zhang, C. Y. 2021. Moon impact crater detection using nested attention mechanism based UNet++. *IEEE Access*, **9**: 44107−44116.

[20] Fairweather, J. H., Lagain, A., Servis, K., et al. 2022. Automatic mapping of small lunar impact craters using LRO-NAC images. *Earth and Space Science*, **9**(7): e2021EA002177.

[21] Kim, J. R., Muller, J. P., van Gasselt, S., et al. 2005. Automated crater detection, a new tool for mars cartography and chronology. *Photogrammetric Engineering & Remote Sensing*, **71**(10): 1205−1217.

[22] Giannakis, I., Bhardwaj, A., Sam, L., et al. 2024. A flexible deep learning crater detection scheme using Segment Anything Model (SAM). *Icarus*, **408**: 115797.

[23] Silburt, A., Ali-Dib, M., Zhu, C. C., et al. 2019. Lunar crater identification via deep learning. *Icarus*, **317**: 27−38.

[24] Herrick, R. R., Bateman, E. M., Crumpacker, W. G., et al. 2018. Observations from a global database of impact craters on Mercury with diameters greater than 5 km. *Journal of Geophysical Research: Planets*, **123**(8): 2089−2109.

[25] Herd, C. D. K., Hamilton, J. S., Walton, E. L., et al. 2024. The source craters of the Martian meteorites: Implications for the igneous evolution of Mars. *Science Advances*, **10**(33): 9.

[26] Osinski, G. R., Grieve, R. A. F., Ferrière, L., et al. 2022. Impact Earth: A review of the terrestrial impact record. *Earth-Science Reviews*, **232**: 104112.

[27] Kenkmann, T. 2021. The terrestrial impact crater record: A statistical analysis of morphologies, structures, ages, lithologies, and more. *Meteoritics & Planetary Science*, **56** (5): 1024−1070.

[28] Crósta, A. P., Silber, E. A., Lopes, R. M. C., et al. 2021. Modeling the formation of Menrva impact crater on Titan: Implications for habitability. *Icarus*, **370**: 114679.

[29] Xiao, Z. Y., Strom, R. G., Chapman, C. R., et al. 2014. Comparisons of fresh complex impact craters on Mercury and the Moon: Implications for controlling factors in impact excavation processes. *Icarus*, **228**: 260−275.
[30] Zhao, Y. Q., Ye, H. X. 2024. Crater detection and population statistics in Tianwen-1 landing area based on Segment Anything Model (SAM). *Remote Sensing*, **16**(10): 1743.
[31] Emami, E., Bebis, G., Nefian, A., et al. 2015. Automatic crater detection using convex grouping and convolutional neural networks. In Advances in Visual Computing. Springer International Publishing, 213–224.
[32] Ali-Dib, M., Menou, K., Jackson, A. P., et al. 2020. Automated crater shape retrieval using weakly-supervised deep learning. *Icarus*, **345**: 113749.
[33] Tewari, A., Prateek, K., Singh, A., et al. 2023. Deep learning-based systems for crater detection: A review. *arXiv: 2310.07727*.
[34] Graettinger, A. H., Boyd, J., Nolan, J. A. 2024. Identification of candidate Martian maars in Arena Colles and Nephentes/Amenthes with extension to maars as a proxy for past groundwater/ice depths. *Icarus*, **426**: 116368.
[35] Daubar, I. J., Garcia, R. F., Stott, A. E., et al. 2024. Seismically detected cratering on Mars: Enhanced recent impact flux? *Science Advances*, **10**(26): 9.
[36] Fairweather, J. H., Lagain, A., Servis, K., et al. 2023. Lunar surface model age derivation: Comparisons between automatic and human crater counting using LRO-NAC and Kaguya TC Images. *Earth and Space Science*, **10**(7): e2023EA002865.
[37] Blanco-Rojas, M., Carroll, M. L., Spradlin, C. S., et al. 2024. A novel approach to impact crater mapping and analysis on Enceladus, using machine learning. *Journal of Geophysical Research: Planets*, **129**(2): 1−12.
[38] Wang, Y. R., Wu, B. 2019. Active machine learning approach for crater detection from planetary imagery and digital elevation models. *IEEE Transactions on Geoscience and Remote Sensing* , **57**(8): 5777−5789.
[39] Kang, Z. Z., Wang, X. K., Hu, T., et al. 2018. Coarse-to-fine extraction of small-scale lunar impact craters from the CCD images of the Chang'E lunar orbiters. *IEEE Transactions on Geoscience and Remote Sensing*, **57**(1): 181−193.
[40] Zang, S. D., Mu, L. L., Xian, L. N., et al. 2021. Semi-supervised deep learning for lunar crater detection using ce-2 dom. *Remote Sensing*, **13**(14): 2819.
[41] Liu, Y. H., Lai, J. L., Xie, M. G, et al. 2024. Identification of lunar craters in the Chang'e-5 landing region based on Kaguya TC Morning Map. *Remote Sensing*, **16**(2): 344.
[42] Lai, Y. F. 2019. A comparison of traditional machine learning and deep learning in image recognition. *Journal of Physics: Conference Series*, **1314**: 012148.
[43] Liao, X. Q., Zheng, H., Wang., H. K., et al. 2024. Performance diagnosis of Oracle database systems based on image encoding and VGG16 model. *IEEE Access*, **12**: 137194−137202.
[44] Siddique, N., Paheding, S., Elkin., C. P., et al. 2021. U-Net and its variants for medical image segmentation: A review of theory and applications. *IEEE Access*, **9**: 82031−82057.
[45] Wang, H., Jiang, J., Zhang, G. J. 2018. CraterIDNet: an end-to-end fully convolutional neural network for crater detection and identification in remotely sensed planetary images. *Remote Sensing*, **10**(7): 1067.
[46] Hong, Z. H., Fan, Z. Y., Zhou, R. Y. 2022. Pyramidal image segmentation based on U-Net for automatic multiscale crater extraction. *Sensors and Materials*, **34**(1): 237−250.
[47] Guo, Y., Wu, H., Yang, S. J., et al. 2024. Crater-DETR: a novel transformer network for crater detection based on dense supervision and multiscale fusion. *IEEE Transactions on Geoscience and Remote Sensing*, **62**: 5614112.
[48] Zhang, Y. N., Kang, Z. Z., Cao, Z. 2024. An image retrieval method for lunar complex craters integrating visual and depth features. *Electronics*, **13**(7): 1262.
[49] Tejas, P., Deep, C., Melissa, M., et al. 2022. Self-supervised learning to guide scientifically relevant categorization of Martian terrain images. In Proceedings of the IEEE/CVF Conference on Computer Vision and Pattern Recognition (CVPR) Workshops.
[50] Xiang, H. Y., Ye, H. X. 2023. Transforming dust storms into clean on Mars images via self supervised learning. In Proceedings of 2023 Cross Strait Radio Science and Wireless Technology Conference.
[51] Lin, X. X., Zhu, Z. W., Yu, X. Y., et al. 2022. Lunar crater detection on digital elevation model: A complete workflow using deep learning and its application. *Remote Sensing*, **14** (3): 621.
[52] Zhang, S. W., Zhang, P., Yang, J. T., et al. 2024. Automatic detection for small-scale lunar impact crater using deep learning. *Advances in Space Research*, **73**(4): 2175−2187.
[53] Yang, H., Xu, X. C., Ma, Y. Q., et al. 2021. CraterdaNet: a convolutional neural network for small-scale crater detection via synthetic-toreal domain adaptation. *IEEE Transactions on Geoscience and Remote Sensing*, **60**: 1−12.
[54] Zou, C., Lai, J. L., Liu, Y. H., et al. 2024. Small lunar crater identification and age estimation in Chang'e-5 landing area based on improved Faster R-CNN. *Icarus*, **410**: 115909.
[55] Chen, D., Hu, F., Mathiopoulos, P. T., et al. 2023. MC-UNet: Martian crater segmentation at semantic and instance levels using U-Net-based convolutional neural network. *Remote Sensing*, **15**(1): 266.
[56] Jia, Y. T., Wan, G., Liu, L., et al. 2021b. Splitattention networks with self-calibrated convolution for moon impact crater dete ction from multi-source data. *Remote Sensing*, **13** (16): 3193.
[57] Xiong, L. Y., Wang, Y. X., Cao, H. Y., et al. 2025. Deep learning detects entire multiple-size lunar craters driven by elevation data and topographic knowledge. *Geo-spatial Information Science*, 1−18.
[58] Zhong, Z. C., Lai, J. L., Zhong, Y. Q., et al. 2025. Enhancing lunar DEM data using super-resolution techniques and optimizing the faster R-CNN network for sub-kilometer crater detection. *Icarus*, **430**: 116483.
[59] Mohite, R. R., Janardan, S. K., Janghel, R. R., et al. 2025. Precision in planetary exploration: Crater detection with residual U-Net34/50 and matching template algorithm. *Planetary and Space Science*, **255**: 106029.
[60] Nan, J., Wang, Y. X., Di, K. C., et al. 2025. YOLOv8-LCNET: an improved YOLOv8 automatic crater detection algorithm and application in the Chang'e-6 landing area. *Sensors*, **25**(1): 243.
[61] Yang, J. T., Zhang, S. W., Li, Lin., et al. 2024. Topographic knowledge-aware network for automatic small-scale impact crater detection from lunar digital elevation models. *International Journal of Applied Earth Observation and Geoinformation*, **129**: 103831.

[62] Ye, P. Q., Hang, R., Xu, Y. S., et al. 2025. 3D morphometry of Martian craters from HRSC DEMs using a multi-scale semantic segmentation network and morphological analysis. *Icarus*, **426**: 116358.
[63] Yu, Z. C., Fong, S., Millham, R. C. 2025. Small-scale Martian Crater Detection by deep learning with enhanced capture of features information and long-range dependencies. *IEEE Geoscience and Remote Sensing Letters*, **22**: 3539947.
[64] Lee, C. 2019. Automated crater detection on Mars using deep learning. *Planetary and Space Science*, **170**: 16−28.
[65] Pedrosa, M. M., de Azevedo, S. C., da Silva, E. A., et al. 2017. Improved automatic impact crater detection on Mars based on morphological image processing and template matching. *Geomatics, Natural Geomatics, Natural Hazards and Risk*, **8**(2): 1306−1319.
[66] Jin, S. G., Zhang, T. Y. 2014. Automatic detection of impact craters on Mars using a modified adaboosting method. *Planetary and Space Science*, **99**: 112−117.
[67] Emmanuel, H., Yu, J. Y., Wang, L. 2023. Object-oriented remote sensing approaches for the detection of terrestrial impact craters as a reconnaissance survey. *Remote Sensing*, **15**(15): 3807.
[68] Head, J., Fassett, J. W., Kadish, C. I., et al. 2010. Global distribution of large lunar craters: Implications for resurfacing and impactor populations. *Science*, **329**(5998): 1504−1507.
[69] Salamunićcar, G., Lončarić, S., Mazarico, E. 2012. LU60645GT and MA132843GT catalogues of Lunar and Martian impact craters developed using a crater shape-based interpolation crater detection algorithm for topography data. *Planetary and Space Science*, **60**(1): 236−247.
[70] Povilaitis, R. Z., Robinson, M. S., Van der Bogert, C. H., et al. 2018. Crater density differences: Exploring regional resurfacing, secondary crater populations, and crater saturation equilibrium on the moon. *Planetary and Space Science*, **162**: 41−51.
[71] Robbins, S. J. 2019. A new global database of lunar impact craters > 1–2 km: 1. Crater locations and sizes, comparisons with published databases, and global analysis. *Geophysical Research: Planets*, **124**(4): 871−892.
[72] Barlow, N. G. 1988. Crater size-frequency distributions and a revised Martian relative chronology. *Icarus*, **75**(2): 285−305.
[73] Kinczyk, M. J., Prockter, L. M., Chapman, C. R., et al. 2016. A morphological evaluation of crater degradation on Mercury: Revisiting crater classification with MESSENGER data. In Proceedings of 45th Lunar and Planetary Science Conference.
[74] Lorenz, R. D., Wood, C. A., Lunine, J. I., et al. 2007. Titan's young surface: Initial impact crater survey by Cassini RADAR and model comparison. *Geophysical Research Letters*, **34**(7): L07204.
[75] Salamunićcar, G., Lončarić, S., Grumpe, A., et al. 2014. Hybrid method for crater detection based on topography reconstruction from optical images and the new LU78287GT catalogue of Lunar impact craters. *Advances in Space Research*, **53**(12): 1783−1797.
[76] Yang, C., Zhao, H. S., Bruzzone, L., et al. 2020. Lunar impact crater identification and age estimation with Chang'E data by deep and transfer learning. *Nature Communications*, **11**: 6358.
[77] Cadogan, P. H. 2020. Automated precision counting of very small craters at lunar landing sites. *Icarus*, **348**: 113822.
[78] Tewari, A., Jain, V., Khanna, N. 2024. Automatic crater shape retrieval using unsupervised and semi-supervised systems. *Icarus*, **408**: 115761.
[79] Stepinski, T. F., Mendenhall, M. P., Bue, B. D., et al. 2009. Machine cataloging of impact craters on Mars. *Icarus*, **203** (1): 77−87.
[80] Lagain, A., Bouley, S., Baratoux, D., et al. 2021. Mars Crater Database: A participative project for the classification of the morphological characteristics of large Martian craters. In Proceedings of Large Meteorite Impacts and Planetary Evolution VI.
[81] Lyapidevskaya, Z. A., Gusiakov, V. K. 2010. Catalog and database on the Earth impact structures. Bulletin of the Novosibirsk Computing Center. *Mathematical Modeling in Geophysics*, **13**: 79−91.
[82] Neish, C. D., Lorenz, R. D. 2012. Titan's global crater population: A new assessment. *Planetary and Space Science*, **60**(1): 26−33.
[83] Jia, Y. T., Su, Z. J., Wan, G., et al. 2023. AE-TransUNet+: An enhanced hybrid transformer network for detection of lunar south small craters in LRO NAC images. *IEEE Geosci Remote Sensing Letters*, 20: 6007405.
[84] Fan, L. L., Yuan, J. B., Zha, K. K., et al. 2022. ELCD: Efficient lunar crater detection based on attention mechanisms and multiscale feature fusion networks from digital elevation models. *Remote Sensing*, **14**(20): 5225.
[85] Hashimoto, S., Mori, K. 2019. Lunar crater detection based on grid partition using deep learning. In Proceedings of 2019 IEEE 13th International Symposium on Applied Computational Intelligence and Informatics (SACI).
[86] Ghilardi, L. 2018. Deep learning semantic segmentation for visionbased hazard detection. Master thesis, Politecnico di Milano.